HHS Public Access

Author manuscript

Muscle Nerve. Author manuscript; available in PMC 2016 July 01.

Published in final edited form as:

Muscle Nerve. 2015 July ; 52(1): 76–82. doi:10.1002/mus.24641.

Analysis of muscle fiber clustering in the diaphragm muscle of sarcopenic mice

Sarah M. Greising[a], **Juan S. Medina-Martínez**[a], **Amrit K. Vasdev**[a], **Gary C. Sieck**[a,b], and **Carlos B. Mantilla**[a,b,*]

[a]Department of Physiology and Biomedical Engineering Mayo Clinic, 200 First Street SW, Rochester, Minnesota 55905, USA

[a]Department of Anesthesiology, Mayo Clinic, 200 First Street SW, Rochester, Minnesota 55905, USA

Abstract

Introduction—Sarcopenia likely comprises muscle fiber denervation and re-innervation, resulting in clustering of muscle fibers of the same type (classified by myosin heavy chain isoform composition). Development of methodology to quantitatively evaluate clustering of muscle fibers according to fiber type is necessary.

Methods—Fiber type specific immunofluorescence histology was used to quantify fiber clustering in murine diaphragm muscle (n=15) at 6 and 24 months of age.

Results—With age, fiber type clustering is evidenced by fiber type specific changes in distances between fibers, specifically a 14% decrease to the closest fiber for type I and 24% increase for type IIx and/or IIb fibers ($P<0.001$). Additionally, a 34% increase to the 3 closest type IIx and/or IIb fibers was found ($P<0.001$).

Discussion—This novel method of analyzing fiber type clustering may be useful in examining pathophysiological conditions of motor unit loss in neuromuscular disorders, myopathies, dystrophies, injuries, or amyotrophic lateral sclerosis.

Keywords

Aging; Cross-sectional area; Fiber type; Motor unit; Myosin heavy chain; Sarcopenia

INTRODUCTION

Sarcopenia is the age-related decline in the skeletal muscle function, including muscle weakness, fiber atrophy, and a reduction in muscle mass.[1] A possible mechanism for this decline in muscle function is the loss of motor units with age.[2–6] Specifically, a motor unit consists of all muscle fibers innervated by a motor neuron; selective loss of motor units is a common feature of sarcopenia across various muscles and species.[7–10] Muscle fiber type is recognized as being determined in large part by motor neuron properties.[11–15] The

*For reprints contact: Carlos B. Mantilla, 200 First Street SW, SMH Jo 4-184, Rochester, MN 55905, mantilla.carlos@mayo.edu, Phone: 1-507-284-7461, Fax: 1-507-255-7300.

classification of motor units is based on the contractile and fatigue properties of the muscle fibers and motor unit classification parallels that of muscle fiber types according to the myosin heavy chain (MyHC) isoform composition.[12, 14–18] Accordingly, muscle fibers within a motor unit express predominantly one type of MyHC isoform and are classified as type I, type IIa and type IIx and/or IIb.

Motor neuron loss in sarcopenia,[4] and resultant muscle fiber denervation and re-innervation by neighboring axons may cause a transition in muscle fiber phenotype. This clustering of muscle fibers of the same type is expected to lead to loss of the normal mosaic pattern of fiber type distribution in adult skeletal muscles. Motor unit loss and muscle fiber type clustering have also been implicated in neuromuscular disorders, muscular dystrophies and non-dystrophic myopathies, injury and trauma to the nervous system; however, there is scant information regarding methods of quantifying fiber type clustering. Accordingly, the ability to quantify fiber type clustering would be beneficial to many areas of research that encounter motor unit pathophysiology.

We have recently shown that the diaphragm muscle (DIAm) undergoes sarcopenia with selective loss of type IIx and/or IIb fibers.[7] Importantly the DIAm comprises all MyHC isoforms and thus may be used to 1) validate a method for quantification of fiber clustering according to fiber type and 2) analyze fiber type clustering in sarcopenia. We hypothesized that sarcopenia results in clustering of muscle fibers of the same type (classified by MyHC isoform composition).

METHODS

Animals

Adult, male mice (strain background C57BL/6 × 129) were bred and maintained at the Mayo Clinic. Two ages of mice were studied at ~6 (n=8) and 24 (n=7) months of age, considered as young and old, respectively. All protocols were approved by the Institutional Animal Care and Use Committee at the Mayo Clinic, in accordance with the National Institutes of Health Guidelines. All mice were anesthetized with an intraperitoneal injection of 90 mg/kg of ketamine and 10 mg/kg of xylazine, and euthanized by exsanguination.

Morphological analyses of DIAm fibers

Harvesting and staining of midcostal DIAm tissue follows previously described methodology.[7,19] Briefly, midcostal DIAm segments were dissected, frozen, and stored at −80 °C until further examination. Each DIAm segment was sectioned cross-sectionally at 10 μm thickness for histological classification of MyHC isoforms. Individual muscle sections were triple-labeled using primary antibodies for MyHC isoforms: anti-$MyHC_{Slow}$ (Vector Labs VP-M667) and anti-$MyHC_{2A}$ (SC-71 obtained from Developmental Studies Hybridoma Bank [DSHB], Iowa City IA) as well as laminin (Sigma L9393) to label the extracellular matrix surrounding all DIAm fibers. These antibodies were selected to facilitate triple-labeling in the same muscle section. The specificity of these MyHC isoform antibodies has been validated in previous studies.[20–23] Of note, the selection of these antibodies is not conducive to analyses of MyHC co-expression; e.g., type I fibers can be

identified as strongly immunoreactive to anti-$MyHC_{Slow}$ and not to anti-$MyHC_{2A}$ whereas type IIa fibers are immunoreactive to anti-$MyHC_{2A}$ and weakly positive to anti-$MyHC_{Slow}$. We validated this approach to fiber type identification by using complementary antibodies in serial muscle sections, including anti-$MyHC_{Slow}$ and anti-$MyHC_{Slow}$ and $MyHC_{2A}$ (BA-F8 and N2-261, respectively, both from DSHB). All sections were incubated with appropriate fluorescently-conjugated secondary antibodies. Histological staining was enhanced with the used of Mouse on Mouse Kit (Vector Labs BMK-2202) following manufacture instructions. An image of each DIAm section was taken by confocal microscope system (Nikon Instruments Inc., Melville, NY) with argon (488 nm) and solid state (405 and 561 nm) lasers for multi-label fluorescence imaging. Confocal images were saved separately for each fluorescence channel as 16-bit grayscale-TIFF files using Nikon C1 software. All images were merged in NIS-Elements software (Nikon Instruments Inc.) and MetaMorph (Molecular Devices LLC., Sunnyvale, CA). For display purposes only images were produced in Adobe Photoshop (Adobe Systems Inc.; San Jose, CA) by down-converting multi-TIFF files to 8-bit single-channel images, without introducing any changes in brightness or contrast.

Analyses of clustering according to fiber type

For each DIAm segment, a single colorized and merged image of each DIAm cross-section was obtained by merging all three fluorescence channels in NIS-Elements. Individual fibers were type-identified based on MyHC isoform expression. A cluster of DIAm fibers was defined by any two or more fibers of the same type that were adjacent. Using the counting tool in NIS-Elements, the number of type-identified fibers per cluster was determined across all imaged DIAm cross-sections. Investigators conducted fiber counts manually and were blinded to fiber type and group for these measurements.

In order to permit automated analyses of fiber clustering, a custom-designed semi-automated tool was developed in MetaMorph to type-identify individual fibers based on MyHC isoform expression. Muscle fibers were singly classified as type I based on the expression of $MyHC_{Slow}$, as type IIa based on $MyHC_{2A}$ expression, and as type IIx and/or IIb based on the absence of expression of the other two isoforms (Figure 1). A manual threshold was applied for each MyHC isoform within individual confocal images of DIAm cross-sections in MetaMorph, creating a mask for all three fiber types in each image. Laminin fluorescence was used to automatically identify individual DIAm fibers by using morphology filters to classify objects (>50 μm^2 for area and 0.5–1.0 for shape factor). This object mask was then used to identify individual type-specific fibers by applying it to a merged confocal image comprising all three thresholded fluorescence channels and segmenting separate objects of each fiber type. Note that type IIa fibers are weakly immunoreactive to the anti-$MyHC_{Slow}$ antibody used for triple labeling, but type I fibers can be uniquely identified by subtracting type IIa fibers. The cross-sectional area and centroid (i.e., the x,y coordinates) were then obtained for each DIAm fiber. No attempt was made to examine co-expression of MyHC expression in this study design.

Using the data obtained from the semi-automated fiber classification in MetaMorph, further automated analysis of fiber type clustering was conducted in MATLAB (The MathWorks

Inc., Natick, MA, 2012). The distance between fibers was calculated for each DIAm fiber, using the fiber centroids. Using customized tools in MATLAB (Figure 1), for each fiber in an image of the DIAm segment, the average distances to the 3 closest fibers and to all other fibers (i.e., the interfiber distance) were obtained, both independent of fiber type and only for fibers of the same type. In addition, the distance to the closest fiber of the same type was calculated. In order to account for potential differences in size and proportion of fibers across age groups, the distance to the 3 closest fibers of the same fiber type was normalized by the DIAm segment- and fiber type-specific average interfiber distance.

Statistical analysis

Data were analyzed using JMP (JMP Pro version 10; SAS Institute Inc., Cary NC). Analysis was conducted between age groups and across fiber types. Chi-squared was used to analyze the distribution of fiber cross-sectional areas. Two-way ANOVA was used to analyze the number of fibers per cluster and the proportion of fibers types for each fiber type and age group. A mixed linear model, with individual animals as a random effect, was used to analyze DIAm cross-sectional area, the average interfiber distance to all fibers and the 3 closest fibers independent of fiber type, the fiber type specific interfiber distance, the closest fiber dependent on fiber type, the 3 closest fibers dependent on fiber type, and the normalized 3 closest fibers. Post-hoc tests were conducted whenever a significant interaction or main effect was determined. Data is presented as mean ± standard error unless otherwise noted, significance was accepted at $P<0.05$.

RESULTS

The DIAm of two age groups of male mice were examined: young (6 months of age) and old (24 months of age). In total, 5767 DIAm fibers were analyzed in 15 mice (mean ± standard error: 384 ± 73 fibers per animal). Overall, 622, 3541, and 1604 fibers were analyzed for type I, type IIa, and type IIx and/or IIb fibers, respectively.

The presence of sarcopenia was first examined by the cross-sectional area of type-identified DIAm fibers. Individual DIAm fibers were consistently identified and classified according to MyHC isoform composition independent of age group (Figure 1).

Sarcopenia of the DIAm

The distribution of fiber cross-sectional areas was significantly shifted in the old mice (Figure 2; $P<0.001$). There was no interaction between fiber type and across age group when analyzed with a mixed linear model (interaction; $P=0.174$). There was a main effect of fiber type ($P<0.001$) such that the IIx and/or IIb fibers were larger than both the type I and type IIa fibers. In young animals the DIAm cross-sectional area was 548.1 ± 57.4, 537.6 ± 54.9, and 834.2 ± 54.9 μm for type I, type IIa, and type IIx and/or IIb fibers, respectively. In contrast the DIAm cross-sectional area of old animals was 530.3 ± 61.8, 538.3 ± 54.6, and 789.2 ± 60.1 μm for type I, type IIa, and type IIx and/or IIb fibers, respectively. However when analyzed as a mean of means (Table 1), there was a trend for an age related decrease in cross-sectional area in type IIx and/or IIb fibers in the old mice.

There was a significant change in fiber type proportions across ages. There was an interaction of age and fiber type ($P<0.001$) such that there was an increase in the proportion of type IIa fibers and a decrease in the proportion of type IIx and/or IIb fibers in the old compared to young mice. Overall, the proportion of type IIa fibers was greater than that of type I or type IIx and/or IIb fibers regardless of age. The proportion of type I, type IIa and type IIx and/or IIb fibers was 10%, 55%, and 35% in young mice compared to 12%, 72%, and 16%, respectively, in old mice (Figure 3).

Clustering of DIAm Fibers According to Type

Several analytical methods were used to determine DIAm fiber clustering according to fiber type. In the first analysis, a cluster of skeletal muscle fibers was defined as two fibers of the same type with adjoining sarcolemma. The total number of fibers in a cluster was showed an interaction across age and fiber type ($P=0.002$). In young animals, the number of fibers per cluster was 1 ± 1, 8 ± 1, and 8 ± 1 for clusters of type I, type IIa, and type IIx and/or IIb fibers, respectively. Type I fibers in the DIAm of young mice were most commonly found in isolation such that there were significantly fewer type I fibers per cluster in the DIAm of young animals compared to the other fiber types. In old animals, the number of fibers per cluster was 2 ± 1, 16 ± 1, and 6 ± 1 for type I, type IIa, and type IIx and/or IIb fibers, respectively. There were significantly more type IIa fibers per cluster in the DIAm of old animals compared to type I and type IIx and/or IIb fibers. Across age groups, there was a significant increase in the number of type IIa fibers per cluster in the old compared to young DIAm, consistent with clustering of these fibers.

Fiber type clustering was further examined by comparing the interfiber distances for type-identified DIAm fibers. Consistent with the predominant type IIa fiber expression in the DIAm and the lack of changes in the fiber cross-sectional area of these fibers across age groups, there were no differences in the average interfiber distance (244.7 ± 8.7 and 245.5 ± 9.3 μm for young and old animals, respectively; $P=0.952$) or the distance to the 3 closest fibers independent of fiber type (32.7 ± 1.3 and 32.5 ± 1.4 μm for young and old animals, respectively; $P=0.927$). When examining fibers of the same type, the average interfiber distance is likely influenced by fiber type-specific differences in fiber dimensions (cross-sectional area) and the proportion of the different fiber types. In agreement, there was a significant interaction between age and fiber type on the type-specific average interfiber distance ($P=0.005$; Table 2). There was a significant difference in the average interfiber distance between type I, type IIa, and type IIx and/or IIb fibers in both age groups. However, there were no significant differences in the average interfiber distance across age groups for each fiber type. The average interfiber distance for type I fibers was 6–16% greater than that for type IIa and type IIx and/or IIb fibers.

Fibers in the DIAm are consistently arranged in a hexagonal array such that each fiber is surrounded by 6 fibers. In order to minimize the possible effect of fibers on the thoracic or abdominal surfaces, the distance to the single closest and 3 closest fibers of the same type was determined. In both young and old animals, the average distance to the closest fiber of the same type was ~2-fold greater for type I fibers than for type IIa and for type IIx and/or IIb fibers (Figure 4). There was a significant interaction between age and fiber type

(P<0.001). The average distance to the closest fiber for type IIa fibers was similar across age groups. However, there were differences in the distance to the closest fiber of the same type for type I and type IIx and/or IIb fibers across age groups. The average distance to the closest fiber decreased for type I fibers where as it increased for type IIx and/or IIb fibers in the DIAm of old mice compared to young mice. In light of the aging effects on fiber type proportions, these changes in the distance to the single closest fiber of the same type are consistent with a clustering of type IIa and possibly type I fibers, and greater isolation (declustering) of type IIx and/or IIb fibers.

Analyses were also conducted for the distance to the 3 closest fibers of the same type. There was a significant interaction between age and fiber type (P<0.001; Figure 4). The distance to the 3 closest fibers was greater for type I fibers than for all other fibers in both age groups. For type IIa fibers, the average distance to the 3 closest fibers of the same type was similar to the distance to the 3 closest fibers of any type (~33 μm), consistent with the greater abundance of these fibers in the mouse DIAm. There were no differences in the average distance to the 3 closest fibers of the same type for type I or IIa fibers across age groups. However, there was an increase in the distance to the 3 closest fibers for type IIx and/or IIb fibers with age. Taken together, these results suggest that evaluating clustering of type IIa fibers may be challenging given differences in their relative abundance in the DIAm across age groups. To account for age-related differences in size and proportion of fibers, the distance to the 3 closest fibers of the same fiber type was normalized by the DIAm segment- and fiber type-specific average interfiber distance. In agreement with the fiber type specific distance to the 3 closest fibers, there was a significant interaction between age and fiber type (P<0.001; Figure 4). The normalized distance to the 3 closest fibers for type IIx and/or IIb fibers of young animals was significantly greater than in the old group. For type IIx and/or IIb fibers, the increase in both the distance to the 3 closest fibers and the normalized distance is indicative of the fiber atrophy associated with age and declustering.

DISCUSSION

The purpose of this study was to first develop a method to quantitatively determine muscle fiber type clustering in skeletal muscle. In models of advanced sarcopenia, muscle fiber type clustering has been reported.[3,24] However, most reports to date have only qualitatively described the presence of fiber type clustering as a change in the normal mosaic pattern of fiber distribution in adult skeletal muscle. The DIAm was selected given that it is of mixed fiber type composition and sarcopenia is associated with a fiber type selective reduction in the proportion and size of muscle fibers that is restricted to type IIx and/or IIb fibers,[7] consistent with selective loss of these motor neurons. We hypothesized that sarcopenia results in clustering of muscle fibers of the same type reflecting denervation of type IIx and/or IIb fibers followed by re-innervation of these muscle fibers by neighboring axons.

Consistent with previous results,[6,7,22,23] type IIx and/or IIb DIAm fibers were found to be ~50% larger than type I and type IIa fibers across age groups. By 24 months of age, the cross-sectional area of type IIx and/or IIb fibers decreased, consistent with selective atrophy of these fibers in sarcopenic rats[3] and mice.[7] In 24 month old mice, the distribution of DIAm fiber cross-sectional areas showed a leftward shift, reflecting reduced size and fewer

numbers of the largest muscle fibers (type IIx and/or IIb). Although the present study examined the mouse DIAm, the proportion of type IIx and/or IIb fibers decreases in the soleus, DIAm, quadriceps, and gastrocnemius muscles of older rats, mice and humans.[7,9,25,26]

Several results from the present study support clustering of fibers according to fiber type in old age. The proportion of type IIa fibers increased, possibly reflecting reinnervation of neighboring denervated type IIx and/or IIb fibers by the most abundant type IIa fibers. In agreement, the number of fibers per cluster increased for type IIa fibers in old mice. Furthermore, the distance to the closest fibers of the same type for type IIx and/or IIb fibers increased in old age whereas that for type I fibers either decreased or was unchanged (following normalization for differences in fiber distribution and size across groups). The distance to the closest fibers of the same type for type IIa fibers was not impacted, reflecting the abundance of type IIa fibers (i.e., the closest fiber to any IIa fiber would likely be another IIa fiber).

The effects of denervation and re-innervation have also been implicated in various neuromuscular disorders, injury and trauma to the nervous system.[17,26–29] For example, in surgically re-innervated muscles there is increased intramuscular sprouting of regenerating axons and qualitative descriptions of muscle fiber type clustering.[30–33] Seminal studies examining cross-innervation of skeletal muscles of predominantly different fiber type composition (i.e., the soleus and the flexor digitorum longus muscles) provide clear physiologic evidence of contractile and metabolic adaptations consistent with those of motor units supplying the re-innervation.[32,33] Selective atrophy of type II fibers, as found in sarcopenia, is evident following denervation,[34] corticosteroid administration,[35] and spinal cord injury[36]. Differences in fiber type proportions were only evident in sarcopenia and denervation,[34,37] suggesting that there might be changes in clustering of fiber types. The methodology developed in this report will permit quantitative evaluation of fiber clustering across any of these conditions and thus facilitate mechanistic interpretation of the fiber type specific changes across motor unit disorders.

In the present study, DIAm fibers were classified based on the predominant MyHC isoform expression in the same muscle section using a semi-automated method. Several studies support a predominant isoform composition in single DIAm fibers.[23,38] However, in various pathophysiological conditions of skeletal muscle atrophy, there is evidence of MyHC co-expression in single DIAm fibers, including following denervation or hypothyroidism.[39–41] The selection of antibodies used in this paper permitted triple labeling of mouse samples, but precluded analyses of co-expression. Indeed, it is possible that co-expression of $MyHC_{2X}$ or $MyHC_{2B}$ with either $MyHC_{Slow}$ and $MyHC_{2A}$ is present in the sarcopenic DIAm. In the present study, there was no evidence of increased difficulty in fiber type classification (i.e., thresholding effects on object classification) in the DIAm of old mice, suggesting that co-expression of $MyHC_{Slow}$ and $MyHC_{2A}$, even if present, was minimal. Future studies must carefully consider the selection of antibodies used for the semi-automated fiber type classification and clustering analyses.

This novel method of quantifying the spatial distribution of type-identified DIAm fibers showed clustering of fibers of the same type with sarcopenia. Collectively, the results of the present study support clustering of type I and type IIa fibers through the increase in distances in type IIx and/or IIb fibers during DIAm sarcopenia. The methodology developed to quantitatively evaluate clustering of fibers according to fiber type was thus validated using a well-established model of sarcopenia in the DIAm. Further investigation into fiber type clustering in other muscle groups and in across a spectrum of neuromuscular diseases may now be accomplished with this quantitative methodology.

Acknowledgement

This research was supported by grants from National Institute of Health R01-AG044615 (CBM & GCS) and T32-HL105355 (SMG), and the Mayo Clinic.

Abbreviations

DIAm	diaphragm muscle
MyHC	myosin heavy chain

References

1. Fielding RA, Vellas B, Evans WJ, Bhasin S, Morley JE, Newman AB, Abellan van Kan G, Andrieu S, Bauer J, Breuille D, Cederholm T, Chandler J, De Meynard C, Donini L, Harris T, Kannt A, Keime Guibert F, Onder G, Papanicolaou D, Rolland Y, Rooks D, Sieber C, Souhami E, Verlaan S, Zamboni M. Sarcopenia: an undiagnosed condition in older adults. Current consensus definition: prevalence, etiology, and consequences. International working group on sarcopenia. J Am Med Dir Assoc. 2011; 12(4):249–256. [PubMed: 21527165]
2. Buford TW, Anton SD, Judge AR, Marzetti E, Wohlgemuth SE, Carter CS, Leeuwenburgh C, Pahor M, Manini TM. Models of accelerated sarcopenia: critical pieces for solving the puzzle of age-related muscle atrophy. Ageing Res Rev. 2010; 9(4):369–383. [PubMed: 20438881]
3. Kung TA, Cederna PS, van der Meulen JH, Urbanchek MG, Kuzon WM Jr, Faulkner JA. Motor unit changes seen with skeletal muscle sarcopenia in oldest old rats. The journals of gerontology Series A, Biological sciences and medical sciences. 2014; 69(6):657–665.
4. Drey M, Krieger B, Sieber CC, Bauer JM, Hettwer S, Bertsch T. Motoneuron loss is associated with sarcopenia. J Am Med Dir Assoc. 2014; 15(6):435–439. [PubMed: 24656689]
5. Cozzoli A, Capogrosso RF, Sblendorio VT, Dinardo MM, Jagerschmidt C, Namour F, Camerino GM, De Luca A. GLPG0492, a novel selective androgen receptor modulator, improves muscle performance in the exercised-mdx mouse model of muscular dystrophy. Pharmacol Res. 2013; 72:9–24. [PubMed: 23523664]
6. Gawel M, Kostera-Pruszczyk A. Effect of age and gender on the number of motor units in healthy subjects estimated by the multipoint incremental MUNE method. Journal of clinical neurophysiology : official publication of the American Electroencephalographic Society. 2014; 31(3):272–278. [PubMed: 24887612]
7. Greising SM, Mantilla CB, Gorman BA, Ermilov LG, Sieck GC. Diaphragm muscle sarcopenia in aging mice. Experimental Gerontology. 2013; 48(9):881–887. [PubMed: 23792145]
8. Ciciliot S, Rossi AC, Dyar KA, Blaauw B, Schiaffino S. Muscle type and fiber type specificity in muscle wasting. The international journal of biochemistry & cell biology. 2013; 45(10):2191–2199. [PubMed: 23702032]
9. Nilwik R, Snijders T, Leenders M, Groen BB, van Kranenburg J, Verdijk LB, van Loon LJ. The decline in skeletal muscle mass with aging is mainly attributed to a reduction in type II muscle fiber size. Experimental Gerontology. 2013; 48(5):492–498. [PubMed: 23425621]

10. Munson JB, Foehring RC, Lofton SA, Zengel JE, Sypert GW. Plasticity of medial gastrocnemius motor units following cordotomy in the cat. J Neurophysiol. 1986; 55(4):619–634. [PubMed: 3701396]
11. Burke, RE. Motor units: Anatomy, physiology, and functional organization. York, N., editor. Handbook of Physiology: Raven Press; 1975. p. 345-420.
12. Greising SM, Gransee HM, Mantilla CB, Sieck GC. Systems biology of skeletal muscle: fiber type as an organizing principle. Wiley Interdiscip Rev Syst Biol Med. 2012; 4(5):457–473. [PubMed: 22811254]
13. Mantilla CB, Sieck GC. Impact of diaphragm muscle fiber atrophy on neuromotor control. Respir Physiol Neurobiol. 2013; 189(2):411–418. [PubMed: 23831121]
14. Mantilla CB, Sieck GC. Invited Review: Mechanisms underlying motor unit plasticity in the respiratory system. J Appl Physiol. 2003; 94(3):1230–1241. [PubMed: 12571144]
15. Enad JG, Fournier M, Sieck GC. Oxidative capacity and capillary density of diaphragm motor units. J Appl Physiol. 1989; 67(2):620–627. [PubMed: 2529236]
16. Sieck GC, Fournier M, Prakash YS, Blanco CE. Myosin phenotype and SDH enzyme variability among motor unit fibers. J Appl Physiol. 1996; 80(6):2179–2189. [PubMed: 8806928]
17. Sieck GC. Physiological effects of diaphragm muscle denervation and disuse. Clin Chest Med. 1994; 15(4):641–659. [PubMed: 7867280]
18. Fournier M, Sieck GC. Mechanical properties of muscle units in the cat diaphragm. J Neurophysiol. 1988; 59(3):1055–1066. [PubMed: 3367195]
19. Sieck DC, Zhan WZ, Fang YH, Ermilov LG, Sieck GC, Mantilla CB. Structure-activity relationships in rodent diaphragm muscle fibers vs. neuromuscular junctions. Respir Physiol Neurobiol. 2012; 180(1):88–96. [PubMed: 22063925]
20. Schiaffino S, Gorza L, Sartore S, Saggin L, Ausoni S, Vianello M, Gundersen K, Lomo T. Three myosin heavy chain isoforms in type 2 skeletal muscle fibres. J Muscle Res Cell Motil. 1989; 10(3):197–205. [PubMed: 2547831]
21. Radzyukevich TL, Neumann JC, Rindler TN, Oshiro N, Goldhamer DJ, Lingrel JB, Heiny JA. Tissue-specific role of the Na,K-ATPase alpha2 isozyme in skeletal muscle. The Journal of biological chemistry. 2013; 288(2):1226–1237. [PubMed: 23192345]
22. Zhan WZ, Miyata H, Prakash YS, Sieck GC. Metabolic and phenotypic adaptations of diaphragm muscle fibers with inactivation. J Appl Physiol. 1997; 82(4):1145–1153. [PubMed: 9104851]
23. Geiger PC, Cody MJ, Sieck GC. Force-calcium relationship depends on myosin heavy chain and troponin isoforms in rat diaphragm muscle fibers. J Appl Physiol. 1999; 87(5):1894–1900. [PubMed: 10562634]
24. Kanda K, Hashizume K. Changes in properties of the medial gastrocnemius motor units in aging rats. Journal of neurophysiology. 1989; 61(4):737–746. [PubMed: 2656932]
25. Chai RJ, Vukovic J, Dunlop S, Grounds MD, Shavlakadze T. Striking denervation of neuromuscular junctions without lumbar motoneuron loss in geriatric mouse muscle. PloS one. 2011; 6(12):e28090. [PubMed: 22164231]
26. Rowan SL, Rygiel K, Purves-Smith FM, Solbak NM, Turnbull DM, Hepple RT. Denervation causes fiber atrophy and myosin heavy chain co-expression in senescent skeletal muscle. PloS one. 2012; 7(1):e29082. [PubMed: 22235261]
27. Telerman-Toppet N, Coers C. Motor innervation and fiber type pattern in amyotrophic lateral sclerosis and in Charcot-Marie-Tooth disease. Muscle Nerve. 1978; 1(2):133–139. [PubMed: 155778]
28. Baloh RH, Rakowicz W, Gardner R, Pestronk A. Frequent atrophic groups with mixed-type myofibers is distinctive to motor neuron syndromes. Muscle Nerve. 2007; 36(1):107–110. [PubMed: 17299742]
29. Decosterd I, Woolf CJ. Spared nerve injury: an animal model of persistent peripheral neuropathic pain. Pain. 2000; 87(2):149–158. [PubMed: 10924808]
30. Karpati G, Engel WK. Correlative histochemical study of skeletal muscle after suprasegmental denervation, peripheral nerve section, and skeletal fixation. Neurology. 1968; 18(7):681–692. [PubMed: 4233750]

31. Kugelberg E. The motor unit: anatomy and histochemical functional correlations. Riv Patol Nerv Ment. 1976; 97(5):251–258. [PubMed: 146250]
32. Bertelli JA, dos Santos AR, Calixto JB. Is axonal sprouting able to traverse the conjunctival layers of the peripheral nerve? A behavioral, motor, and sensory study of end-to-side nerve anastomosis. Journal of reconstructive microsurgery. 1996; 12(8):559–563. [PubMed: 8951126]
33. Vleggeert-Lankamp CL, de Ruiter GC, Wolfs JF, Pego AP, Feirabend HK, Lakke EA, Malessy MJ. Type grouping in skeletal muscles after experimental reinnervation: another explanation. The European journal of neuroscience. 2005; 21(5):1249–1256. [PubMed: 15813934]
34. Miyata H, Zhan WZ, Prakash YS, Sieck GC. Myoneural interactions affect diaphragm muscle adaptations to inactivity. J Appl Physiol. 1995; 79:1640–1649. [PubMed: 8594024]
35. Lewis MI, Monn SA, Sieck GC. Effect of corticosteroids on diaphragm fatigue, SDH activity, and muscle fiber size. J Appl Physiol. 1992; 72(1):293–301. [PubMed: 1537729]
36. Mantilla CB, Greising SM, Zhan WZ, Seven YB, Sieck GC. Prolonged C2 spinal hemisection-induced inactivity reduces diaphragm muscle specific force with modest, selective atrophy of type IIx and/or IIb fibers. J Appl Physiol. 2013; 114(3):380–386. [PubMed: 23195635]
37. Greising SM, Mantilla CB, Gorman BA, Ermilov LG, Sieck GC. Diaphragm muscle sarcopenia in aging mice. Experimental Gerontology. 2013; 48(9):881–887. [PubMed: 23792145]
38. Geiger PC, Cody MJ, Macken RL, Sieck GC. Maximum specific force depends on myosin heavy chain content in rat diaphragm muscle fibers. J Appl Physiol. 2000; 89(2):695–703. [PubMed: 10926656]
39. Geiger PC, Cody MJ, Han YS, Hunter LW, Zhan WZ, Sieck GC. Effects of hypothyroidism on maximum specific force in rat diaphragm muscle fibers. J Appl Physiol. 2002; 92(4):1506–1514. [PubMed: 11896017]
40. Geiger PC, Cody MJ, Macken RL, Bayrd ME, Sieck GC. Effect of unilateral denervation on maximum specific force in rat diaphragm muscle fibers. J Appl Physiol. 2001; 90(4):1196–1204. [PubMed: 11247914]
41. Mantilla CB, Sieck GC. Neuromuscular adaptations to respiratory muscle inactivity. Respir Physiol Neurobiol. 2009; 169(2):133–140. [PubMed: 19744580]

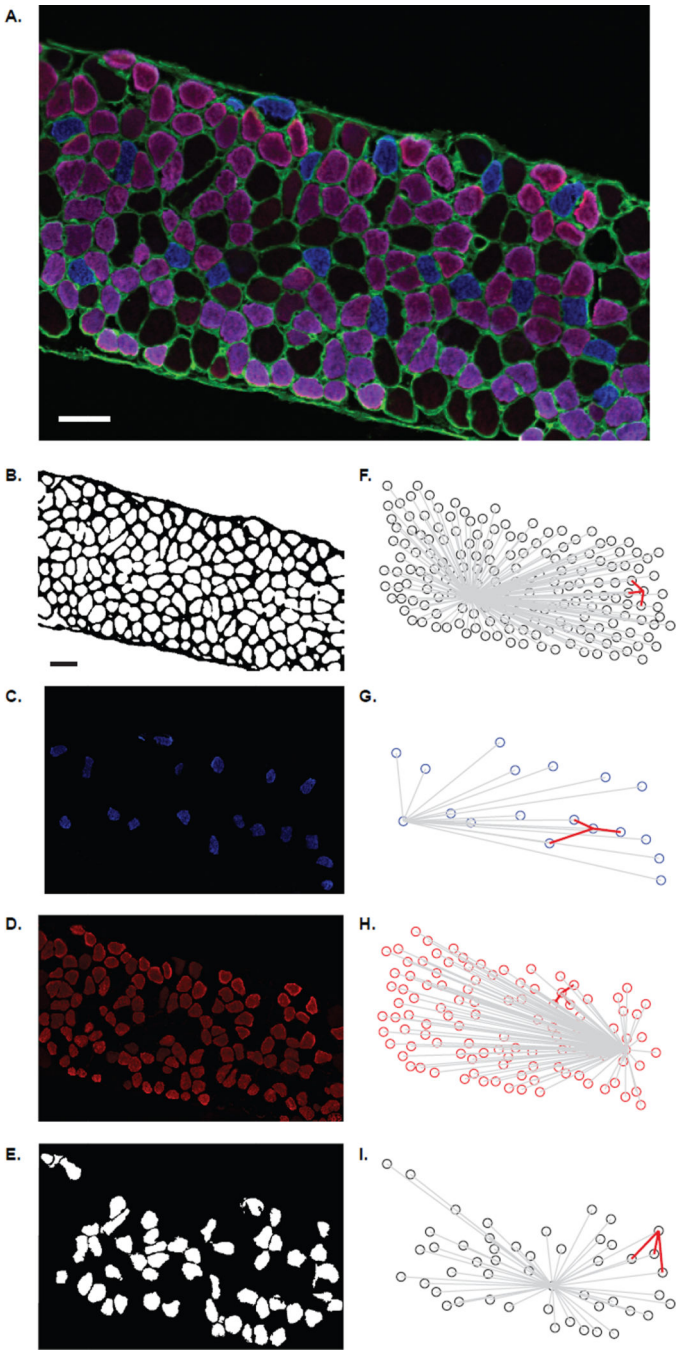

Figure 1.

Representative histologic images as used for analysis of fiber type clustering. **A)** The color combined image of the myosin heavy chain (MyHC) isoforms, blue denotes type I fibers, purple type IIa fibers, and the black type IIx and/or IIb fibers (scale bars are 50 μm). Note that type IIa fibers are weakly immunoreactive to the anti-$MyHC_{Slow}$ antibody used for triple labeling giving a purple hue to type IIa fibers (see Methods). **B)** Using MetaMorph the threshold was set resulting in a black and white image. The black outline is indicative of the sarcolemma of the diaphragm (DIAm) section. The individual fibers types are separated for

analysis; **C)** type I fibers, **D)** type IIa fibers, and **E)** type IIx and/or IIb. The coordinate plots for these figures show the interfiber distance to for all fibers (gray lines) and for the 3 closest fibers (red lines) for a randomly selected fiber. Representative plots are shown for; **F)** all fibers, **G)** type I fibers, **H)** type IIa fibers, and **I)** type IIx and/or IIb.

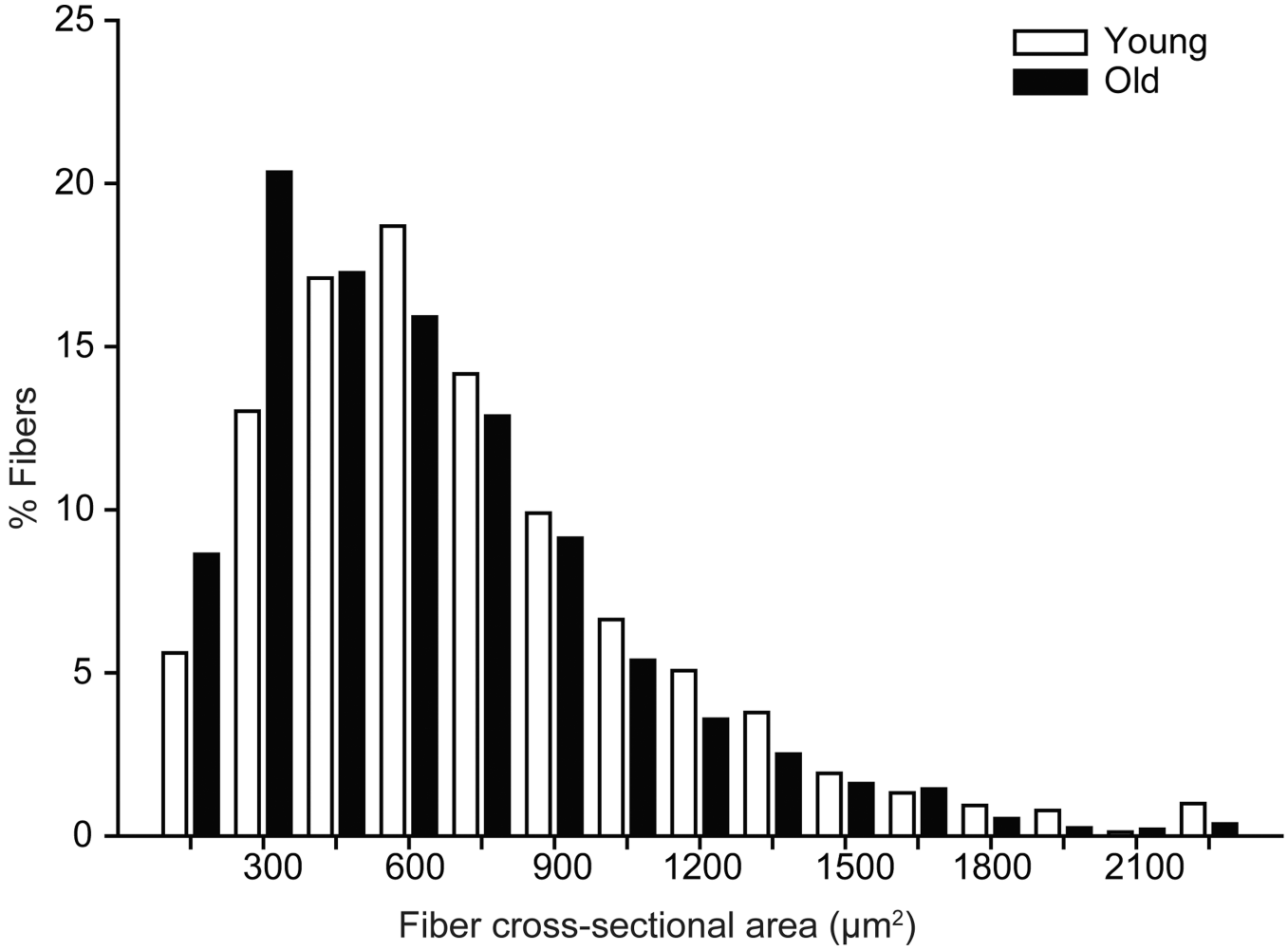

Figure 2.

Diaphragm muscle fiber cross-sectional area from young and old mice, presented as the distribution of fiber cross-sectional areas independent of fiber type. There was a significant left shit in the old fiber cross-sectional areas in comparison to young; distribution was analyzed by chi-squared analysis ($P<0.001$).

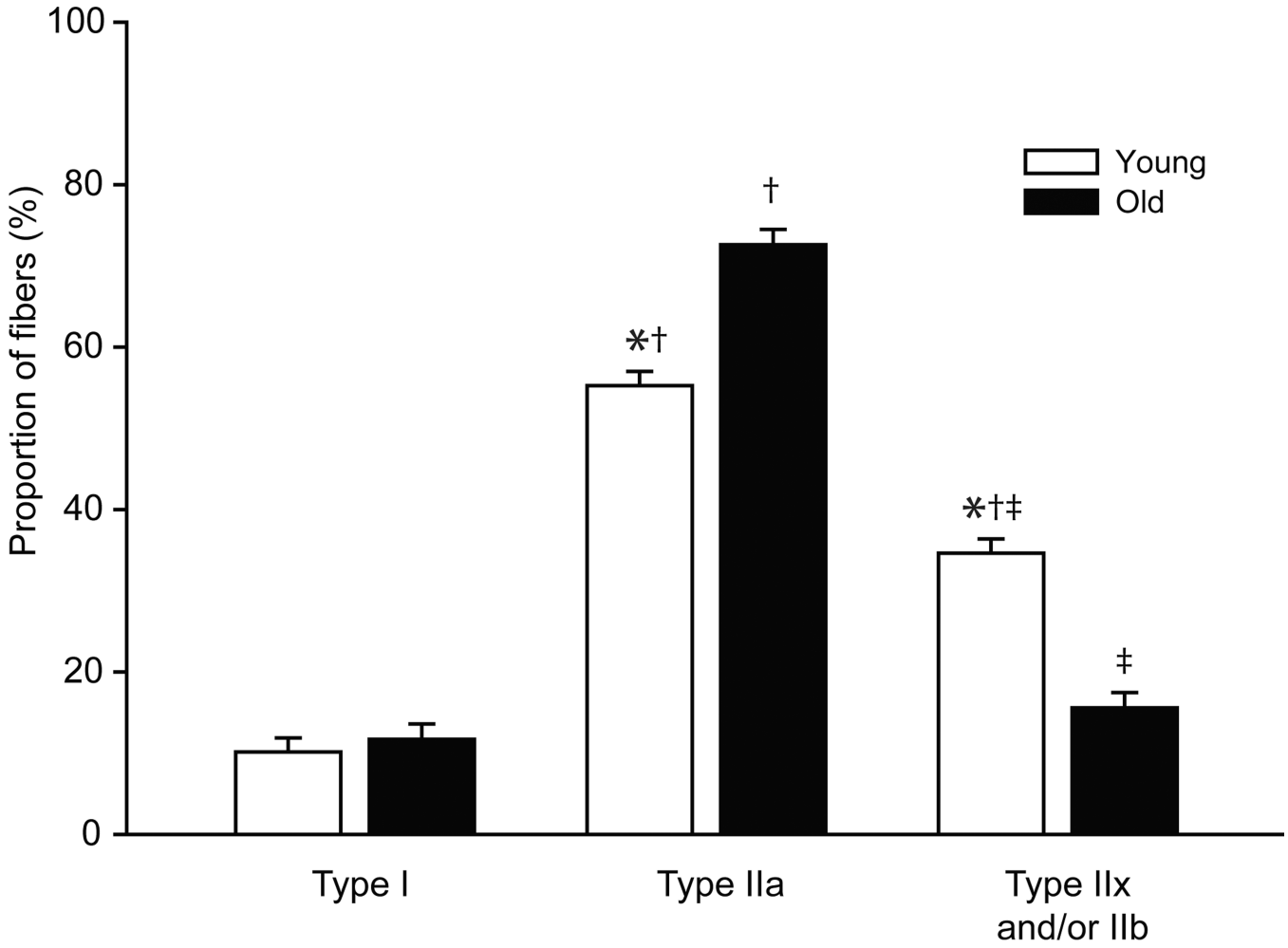

Figure 3.

Diaphragm muscle fiber type proportions from young and old mice. Data were analyzed was analyzed by two-way ANOVA (age×fiber type); there was an interaction of age and fiber type ($P<0.001$). Interaction post hoc results are as follows: *significantly different than old age group of same fiber type; †significantly different than type I fibers; ‡significantly different than type IIa fibers.

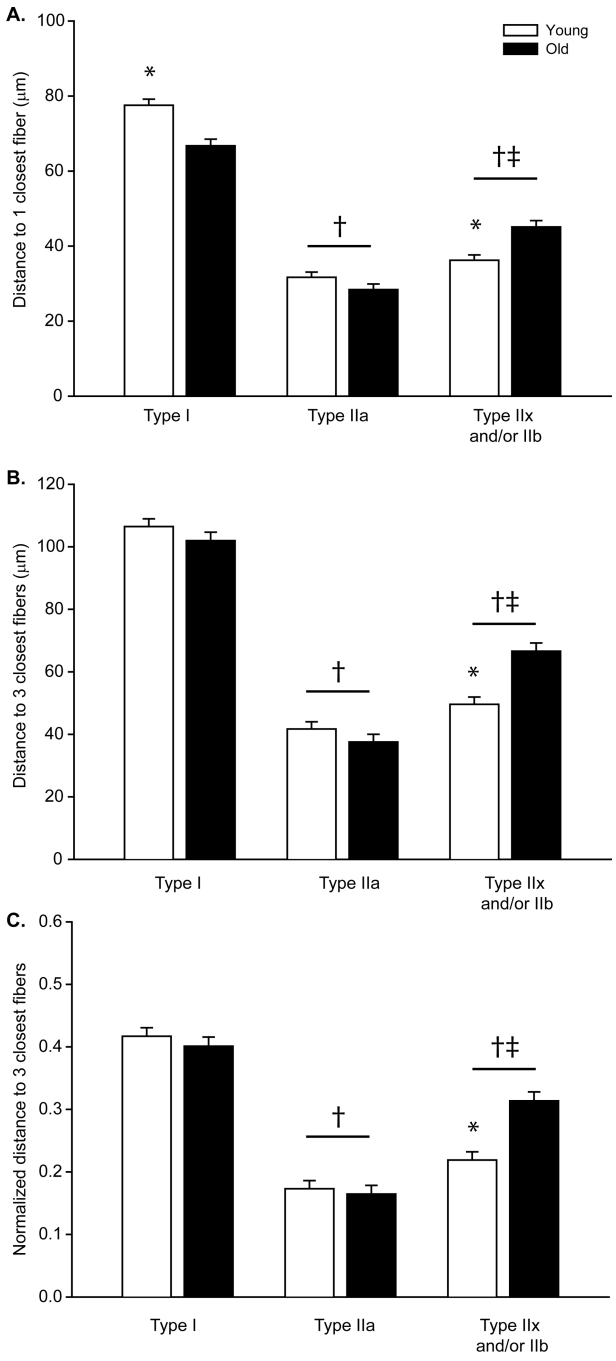

Figure 4.

The type dependent distance to fibers was determined for **A)** the closest individual fiber and **B)** the 3 closest fibers across ages. **C)** The distance to the 3 closest fibers dependent on fiber type was also normalized by the type specific average interfiber distance to account for the change in fiber type proportions with age. Data was analyzed with a mixed linear model with an individual animal as a random effect (age×fiber type×animal); there was a main

effect of age and fiber type P<0.001.*significantly different than old age group of same fiber type; †significantly different than type I fibers; ‡significantly different than type IIa fibers.

Table 1

Fiber type specific cross-sectional area of the diaphragm muscle of young and old mice

	Young	Old
Type I	477.5 ± 62.1	530.2 ± 66.3
Type IIa	520.3 ± 62.1	542.8 ± 66.3
Type IIx and/or IIb*,†	877.9 ± 62.1	781.4 ± 66.3

The DIAm cross-sectional area (μm^2), data was analyzed by the mean of the mean with the individual animal as a random effect (age × fiber type × animal; main effect of age P=0.893, main effect of fiber type P<0.001, interaction P=0.477), data presented as least squared mean ± standard error.

*significantly different from Type I fibers;

†significantly different from type IIa fibers, main effect

Table 2

Fiber type dependent average interfiber distance

	Young	Old
Type I	265.6 ± 9.4	257.0 ± 10.1
Type IIa	248.2 ± 9.0†	245.6 ± 9.6†
Type IIx and/or IIb	233.8 ± 9.1†	216.6 ± 10.0†

Average interfiber distance (μm) was analyzed with a mixed linear model with an individual animal as a random effect (age × fiber type × animal; interaction P=0.005), data are presented as least squared mean ± standard error.

†significantly different than type I fibers of same age group.